PERGAMON

International Journal of Solids and Structures 39 (2002) 4723–4746

INTERNATIONAL JOURNAL OF SOLIDS and STRUCTURES

www.elsevier.com/locate/ijsolstr

A Galerkin boundary integral method for multiple circular elastic inclusions with homogeneously imperfect interfaces

S.G. Mogilevskaya *, S.L. Crouch

Department of Civil Engineering, University of Minnesota, 500 Pillsbury Drive S.E., Minneapolis, MN 55455, USA

Received 30 October 2001; received in revised form 14 May 2002

Abstract

A Galerkin boundary integral method is presented to solve the problem of an infinite, isotropic elastic plane containing a large number of randomly distributed circular elastic inclusions with homogeneously imperfect interfaces. Problems of interest might involve thousands of inclusions with no restrictions on their locations (except that the inclusions may not overlap), sizes, and elastic properties. The tractions are assumed to be continuous across the interfaces and proportional to the corresponding displacement discontinuities. The analysis is based on a numerical solution of a complex hypersingular integral equation with the unknown tractions and displacement discontinuities at each circular boundary approximated by truncated complex Fourier series. The method allows one to calculate the stress and displacement fields everywhere in the matrix and inside the inclusions. Numerical examples are included to demonstrate the effectiveness of the approach.

Keywords: Galerkin boundary integral method; Complex hypersingular integral equation; Multiple circular inclusions; Imperfect interface

1. Introduction

Evaluation of the elastic fields for an array of elastic inclusions within an elastic matrix is important for analysis of micromechanical behavior of fiber-reinforced materials. In a previous paper (Mogilevskaya and Crouch, 2001), we presented a new numerical approach for solving two-dimensional problems involving a large number of circular elastic inclusions in an infinite elastic plane. Problems of interest might involve thousands of inclusions with no restrictions on their locations (except that the inclusions may not overlap), sizes, and elastic properties. The approach allows one to calculate elastic fields everywhere in the matrix and inside the inclusions. The bond between the inclusions and matrix is assumed to be *perfect*, so the tractions and displacements are continuous across the interfaces.

* Corresponding author. Tel.: +1-612-625-4810; fax: +1-612-626-7750.
E-mail address: mogil003@umn.edu (S.G. Mogilevskaya).

0020-7683/02/$ - see front matter
PII: S0020-7683(02)00374-8

The problem of multiple interacting circular inhomogeneities in plane elastostatics has also been considered by Gong and Meguid (1993). Their approach is based on superposition of the Kolosov–Muskhelishvili potentials (Muskhelishvili, 1959) for the individual inclusions, which are expanded in truncated Laurent series. The unknown coefficients in the expansions are determined from the solution of a system of complex algebraic equations. Gong and Meguid used a perturbation technique to solve this system. In this technique, the unknown coefficients are expanded in infinite series with respect to a characteristic parameter. The disadvantage of this technique is that the results may depend on the choice of the characteristic parameter; in the case of closely packed inclusions with large variations in size, convergence of the series will be difficult to achieve. Gong and Meguid do not mention how many terms of the Laurent series are needed to get accurate results. A problem in the field of groundwater flow analogous to the multiple circular elastic inclusion problem has been considered by Janković (1997) and Barnes and Janković (1999) The analytical/numerical approach used by these authors is referred to as the 'analytic element method' (Strack, 1989).

A number of authors have generalized the concept of perfect bonding in an effort to better represent the real behavior of fiber-reinforced materials (see e.g. Aboudi, 1987; Achenbach and Zhu, 1989, 1990; Hashin, 1990, 1991; Jasiuk and Kouider, 1993; Gao, 1995; Ru and Schiavone, 1997; Ru, 1998, 1999; Bigoni et al., 1998; Sudak et al., 1999; Chen, 2001). This work has led to the development of models for *imperfect interfaces*. The simplest models assume that the tractions are continuous across an interface and that the normal and shear displacement discontinuities are proportional to the normal and shear tractions at the interface. The proportionality coefficients are either assumed to be constant along the interface (a homogeneously imperfect interface) or to vary along it (an inhomogeneously imperfect interface).

Closed-form solutions are available for the problem of a single circular inclusion with an imperfect interface under general loading conditions. Gao (1995), for example, gave the solution for a circular inclusion with a general homogeneously imperfect interface (nonzero normal and shear proportionality coefficients) under the condition of a general two-dimensional eigenstrain and uniform tension at infinity. The same problem was solved analytically by Bigoni et al. (1998) for more general loading conditions at infinity. Solutions for a circular inclusion with an inhomogeneous interface were obtained by Ru (1998) for a sliding interface, Ru and Schiavone (1997) for antiplane shear, Sudak et al. (1999) for an inhomogeneously imperfect interface with equal normal and shear constants, and Chen (2001) for uniform thermal loading.

To the authors' knowledge, the general problem of multiple, randomly distributed, circular elastic inclusions with imperfect interfaces has been considered only using effective medium theories (e.g. Jun and Jasiuk, 1993 for sliding interfaces) or under simplifying assumptions of dilute inclusions when the concentration of the inclusions is very small (e.g. Bigoni et al., 1998). Periodically spaced inclusions were considered in Achenbach and Zhu (1989, 1990). In the present paper we extend a general approach suggested in Mogilevskaya and Crouch (2001) to the case of an infinite elastic plane with a large number of randomly spaced circular inclusions with homogeneously imperfect interfaces under arbitrary biaxial loading at infinity.

2. Problem formulation

Consider an infinite, isotropic elastic plane subjected to a biaxial stress field at infinity and containing N circular elastic inclusions (Fig. 1). The elastic properties of the inclusions (their shear moduli μ_j and Poisson's ratios ν_j, $j = 1, \ldots, N$) are arbitrary and in general are different from those of the matrix μ and ν. The bond between the inclusions and the surrounding material (the matrix) is assumed to be homogeneously imperfect, which means that the normal and shear components of displacement discontinuity across the interface of the jth inclusion are proportional to the corresponding components of traction, i.e.

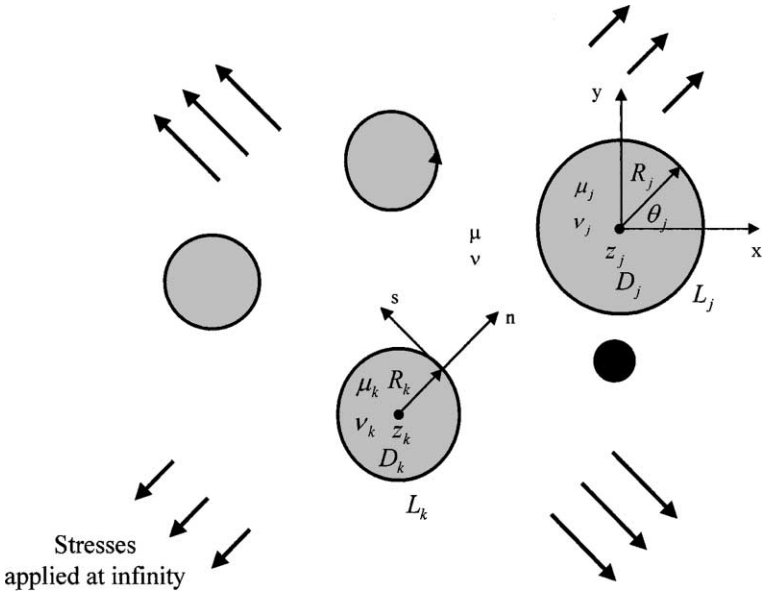

Fig. 1. Problem formulation.

$$\Delta u_{jn} = -\lambda_{jn}\sigma_{jn}, \qquad \Delta u_{js} = -\lambda_{js}\sigma_{js} \tag{1}$$

where $\Delta u_{jn} = (u_{jn})^{\text{inclusion}} - (u_{jn})^{\text{matrix}}$ and $\Delta u_{js} = (u_{js})^{\text{inclusion}} - (u_{js})^{\text{matrix}}$. The positive proportionality constants $(\lambda_{jn}, \lambda_{js})$ in (1) may be different for each inclusion, and perfect bonding occurs when $\lambda_{jn} = \lambda_{js} = 0$. The inclusions may not touch one another, but the distance between them can be arbitrary small. The distribution of displacements and stresses in the composite solid are to be determined. Let R_j, z_j, and L_j denote the radius, center, and boundary of the jth inclusion, D_j. The direction of travel is counterclockwise for all the boundaries L_j. The unit normal n points to the right of the direction of travel (i.e. away from the inclusions); the unit tangent s is directed in the direction of travel.

The system of inclusions is in equilibrium and it follows that the resultant force and moment on the boundary of each inclusion ($j = 1, \ldots, N$) are equal to zero. The mathematical expressions for these conditions can be written as follows (Muskhelishvili, 1959):

$$\int_{L_j} \sigma_j(\tau)\,\mathrm{d}\tau = 0 \tag{2}$$

$$\mathrm{Re}\int_{L_j} \tau\overline{\sigma_j(\tau)}\,\mathrm{d}\bar{\tau} = 0 \tag{3}$$

where $\sigma_j(z) = \sigma_{jn}(z) + \mathrm{i}\sigma_{js}(z)$, $z = x + \mathrm{i}y$ is complex coordinate of a point (x, y) in the global Cartesian coordinate system (xOy) in a plane, with, of course, $\mathrm{i} = \sqrt{-1}$.

3. Boundary integral equation

The problem formulated above is a particular case of a more general problem of an infinite plane or a finite body containing cracks, cavities, and inclusions of arbitrary shapes. The complex hypersingular

boundary integral equation governing this general problem is given in Linkov and Mogilevskaya (1994). For the particular case considered here this equation can be written as follows:

$$\sum_{j=1}^{N}\left[2\int_{L_j}\frac{\Delta u_j(\tau)}{(\tau-t)^2}\,\mathrm{d}\tau-\int_{L_j}\Delta u_j(\tau)\frac{\partial}{\partial t}\,\mathrm{d}K_1(\tau,t)-\int_{L_j}\overline{\Delta u_j(\tau)}\frac{\partial}{\partial t}\,\mathrm{d}K_2(\tau,t)+(2a_{1j}-a_{3j})\int_{L_j}\frac{\sigma_j(\tau)\,\mathrm{d}\tau}{\tau-t}\right.$$
$$\left.+(a_{1j}-a_{3j})\int_{L_j}\sigma_j(\tau)\frac{\partial}{\partial t}K_1(\tau,t)\,\mathrm{d}\tau+a_{1j}\int_{L_j}\overline{\sigma_j(\tau)}\frac{\partial}{\partial t}K_2(\tau,t)\,\mathrm{d}\bar{\tau}\right]=2\pi i\left[\frac{a_2}{2}\sigma(t)+\sigma^{\infty}(t)\right] \tag{4}$$

where $t\in\cup_{j=1}^{N}L_j$, $\Delta u_j=\Delta u_{jx}+i\Delta u_{jy}$; Δu_{jx} and Δu_{jy} are displacement discontinuity components in directions Ox and Oy respectively;

$$\left.\begin{array}{l}a_2=a_{2j}\\ \sigma(t)=\sigma_j(t)\end{array}\right\}\quad\text{if } t\in L_j \tag{5}$$

$$a_{1j}=\frac{1}{2\mu_j}-\frac{1}{2\mu};\qquad a_{2j}=\frac{1+\kappa_j}{2\mu_j}+\frac{1+\kappa}{2\mu};\qquad a_{3j}=\frac{1+\kappa_j}{2\mu_j}-\frac{1+\kappa}{2\mu} \tag{6}$$

$$\sigma^{\infty}(t)=-\frac{\kappa+1}{4\mu}\left[\sigma_{xx}^{\infty}+\sigma_{yy}^{\infty}+\frac{\mathrm{d}\bar{t}}{\mathrm{d}t}(\sigma_{yy}^{\infty}-\sigma_{xx}^{\infty}-2i\sigma_{xy}^{\infty})\right] \tag{7}$$

σ_{xx}^{∞}, σ_{yy}^{∞}, and σ_{xy}^{∞} are the stresses at infinity; $\kappa=3-4\nu$ in plane strain; $\kappa=(3-\nu)/(1+\nu)$ in plane stress; a bar over a symbol denotes complex conjugation; $\mathrm{d}\bar{t}/\mathrm{d}t=\exp(-2i\gamma)$ where γ is the angle between the axis Ox and tangent at the point t; and

$$K_1(\tau,t)=\ln\frac{\tau-t}{\bar{\tau}-\bar{t}};\qquad K_2(\tau,t)=\frac{\tau-t}{\bar{\tau}-\bar{t}}$$

In the case of perfect bonding $\Delta u_j=0$ for $j=1,\ldots,N$ and Eq. (4) reduces to the one considered in Mogilevskaya and Crouch (2001).

The components of the stress tensor σ_{xx}, σ_{yy}, and σ_{xy} and the displacements $u(z)$ at any point z inside the inclusions and matrix can be calculated from two complex functions $\varphi(z)$ and $\psi(z)$ by using the Kolosov–Muskhelishvili formulae (Muskhelishvili, 1959)

$$\begin{array}{l}2\mu u(z)=\kappa\varphi(z)-z\overline{\varphi'(z)}-\overline{\psi(z)}\\ \sigma_{xx}+\sigma_{yy}=4\,\mathrm{Re}\,\varphi'(z)\\ \sigma_{yy}-\sigma_{xx}+2i\sigma_{xy}=2[\bar{z}\varphi''(z)+\psi'(z)]\end{array} \tag{8}$$

The Kolosov–Muskhelishvili potentials can be expressed in terms of integrals of the boundary tractions and displacement discontinuities as follows (see e.g. Wang et al., 2001):

$$\varphi(z)=-\frac{\mu_l}{\pi i(\kappa_l+1)}\sum_{j=1}^{N}\left[a_{1j}\int_{L_j}\sigma_j(\tau)\ln(\tau-z)\,\mathrm{d}\tau-\int_{L_j}\frac{\Delta u_j(\tau)\,\mathrm{d}\tau}{\tau-z}\right]+\varphi^{\infty}(z)$$
$$\psi(z)=-\frac{\mu_l}{\pi i(\kappa_l+1)}\sum_{j=1}^{N}\left\{a_{1j}\int_{L_j}\sigma_j(\tau)\frac{\bar{\tau}\,\mathrm{d}\tau}{\tau-z}+(a_{3j}-a_{1j})\int_{L_j}\overline{\sigma_j(\tau)}\ln(\tau-z)\,\mathrm{d}\bar{\tau}\right. \tag{9}$$
$$\left.-\int_{L_j}\frac{\Delta u_j(\tau)\,\mathrm{d}\bar{\tau}}{\tau-z}+\int_{L_j}\frac{\overline{\Delta u}_j(\tau)\,\mathrm{d}\tau}{\tau-z}+\int_{L_j}\frac{\Delta u_j(\tau)}{(\tau-z)^2}\bar{\tau}\,\mathrm{d}\tau\right\}+\psi^{\infty}(z)$$

where μ_l, κ_l are the elastic constants of the lth inclusion if $z\in D_l$, and $\mu_l=\mu$, $\kappa_l=\kappa$ if z is a point of the matrix, and

$$\varphi^{\infty}(z) = \frac{\mu_l(\kappa+1)}{\mu(\kappa_l+1)}\frac{\sigma_{xx}^{\infty}+\sigma_{yy}^{\infty}}{4}z$$
$$\psi^{\infty}(z) = \frac{\mu_l(\kappa+1)}{\mu(\kappa_l+1)}\frac{\sigma_{yy}^{\infty}-\sigma_{xx}^{\infty}+2i\sigma_{xy}^{\infty}}{2}z \tag{10}$$

4. Numerical solution

4.1. Approximation of the unknown functions

In order to solve (4), we represent the unknown tractions $\sigma_j(\tau)$ at each boundary L_j by a truncated complex Fourier series of the form

$$\sigma_j(\tau) \approx \sum_{m=1}^{M_{1j}} B_{-mj}F_{mj} + \sum_{m=0}^{M_{2j}} B_{mj}/F_{mj}, \quad \tau \in L_j \tag{11}$$

where

$$F_{mj}(\tau) = \left(\frac{R_j}{\tau - z_j}\right)^m \tag{12}$$

By substituting the expression (11) into equilibrium conditions (2) and (3), and using the main integral theorems of the theory of complex variables, we find that

$$B_{-1j} = 0; \quad B_{0j} \text{ are real} \tag{13}$$

for all $j = 1, \ldots, N$. We noted previously (Mogilevskaya and Crouch, 2001) that the equilibrium conditions are introduced merely to simplify subsequent derivations. Conditions (13) would follow automatically from the solution of (4) because this equation requires no additional conditions for the solution to exist (Linkov and Mogilevskaya, 1995).

Using standard formulae for the change of variables (θ_j is shown in Fig. 1)

$$\Delta u_{jx} = \Delta u_{jn}\cos\theta_j - \Delta u_{js}\sin\theta_j$$

$$\Delta u_{jy} = \Delta u_{jn}\sin\theta_j + \Delta u_{js}\cos\theta_j$$

and the relation

$$\exp(i\theta_j) = \cos\theta_j + i\sin\theta_j = \frac{\tau - z_j}{R_j}$$

we get from expressions (1) the following representation of the displacement discontinuities $\Delta u_j(\tau)$

$$\Delta u_j(\tau) = -\frac{\tau - z_j}{R_j}(\alpha_j\sigma_j + \beta_j\bar{\sigma}_j) \tag{14}$$

where

$$\alpha_j = 0.5(\lambda_{jn} + \lambda_{js}); \qquad \beta_j = 0.5(\lambda_{jn} - \lambda_{js}) \tag{15}$$

Using expressions (11) and (14) we get

$$\Delta u_j(\tau) \approx -\alpha_j\left[\sum_{m=1}^{M_{1j}} B_{-mj}F_{(m-1)j}(\tau) + \sum_{m=0}^{M_{2j}} B_{mj}/F_{(m+1)j}(\tau)\right] - \beta_j\left[\sum_{m=1}^{M_{1j}} \overline{B}_{-mj}/F_{(m+1)j}(\tau) + \sum_{m=0}^{M_{2j}} \overline{B}_{mj}F_{(m-1)j}(\tau)\right],$$
$$\tau \in L_j \tag{16}$$

The complex coefficients B_{-mj} $(m = 1, \ldots, M_{1j})$ and B_{mj} $(m = 0, \ldots, M_{2j})$ in series (11) and (16) need to be determined. As discussed below, this is accomplished by setting up and solving a system of simultaneous, linear algebraic equations. We note here that the number of coefficients need not be the same for all the individual inclusions.

4.2. Calculation of the integrals

Six types of integrals are involved in (4). The three integrals involving tractions $\sigma_j(\tau)$ are evaluated in our previous paper (Mogilevskaya and Crouch, 2001) and are given as follows for the case in which the evaluation point $t \in L_k$:

$$\begin{aligned}
&\sum_{j=1}^{N}(2a_{1j}-a_{3j})\int_{L_j}\frac{\sigma_j(\tau)\,\mathrm{d}\tau}{\tau-t} = (2a_{1k}-a_{3k})\pi i\left[-\sum_{m=2}^{M_{1k}}B_{-mk}F_{mk}(t)+\sum_{m=0}^{M_{2k}}B_{mk}/F_{mk}(t)\right]\\
&\qquad\qquad -2\pi i\sum_{\substack{j=1\\ j\neq k}}^{N}(2a_{1j}-a_{3j})\sum_{m=2}^{M_{1j}}B_{-mj}F_{mj}(t)\\
&\sum_{j=1}^{N}(a_{1j}-a_{3j})\int_{L_j}\sigma_j(\tau)\frac{\partial}{\partial t}K_1(\tau,t)\,\mathrm{d}\tau = 2\pi i\sum_{\substack{j=1\\ j\neq k}}^{N}(a_{1j}-a_{3j})\left[\sum_{m=2}^{M_{1j}}B_{-mj}F_{mj}(t)+\sum_{m=0}^{M_{2j}}B_{mj}F_{2k}(t)\overline{F_{(m+2)j}(t)}\right]\\
&\sum_{j=1}^{N}a_{1j}\int_{L_j}\overline{\sigma_j(\tau)}\frac{\partial}{\partial t}K_2(\tau,t)\,\mathrm{d}\bar{\tau} = 2\pi i a_{1k}B_{0k}+2\pi i\sum_{\substack{j=1\\ j\neq k}}^{N}a_{1j}\left[\sum_{m=2}^{M_{1j}}\overline{B}_{-mj}(t)\overline{F_{mj}(t)}\Lambda(t)+B_{0j}F_{2k}(t)\overline{F_{2j}(t)}\right]
\end{aligned} \tag{17}$$

where

$$\Lambda(t) = -1+(m+1)F_{2k}(t)\overline{F_{2j}(t)}-mF_{2k}(t)\frac{t-z_j}{\bar{t}-\bar{z}_j}$$

The integrals involving displacement discontinuities $\Delta u_j(\tau)$ can be calculated analytically in an analogous way using three basic integrals (Appendix A). For the case in which the evaluation point $t \in L_k$, we have

$$\begin{aligned}
\sum_{j=1}^{N}\int_{L_j}\frac{\Delta u_j(\tau)\,\mathrm{d}\tau}{(\tau-t)^2} = -\pi i\Bigg\{&\frac{\alpha_k}{R_k}\left[\sum_{m=2}^{M_{1k}}B_{-mk}(m-1)F_{mk}(t)+\sum_{m=0}^{M_{2k}}B_{mk}(m+1)/F_{mk}(t)\right]\\
&+\frac{\beta_k}{R_k}\left[\sum_{m=2}^{M_{1k}}\overline{B}_{-mk}(m+1)/F_{mk}(t)+\sum_{m=1}^{M_{2k}}\overline{B}_{mk}(m-1)F_{mk}(t)+B_{0k}\right]\\
&+2\sum_{\substack{j=1\\ j\neq k}}^{N}\left[\frac{\alpha_j}{R_j}\sum_{m=2}^{M_{1j}}B_{-mj}(m-1)F_{mj}(t)+\frac{\beta_j}{R_j}\sum_{m=1}^{M_{2j}}\overline{B}_{mj}(m-1)F_{mj}(t)\right]\Bigg\}
\end{aligned}$$

$$\sum_{j=1}^{N}\int_{L_j}\Delta u_j(\tau)\frac{\partial}{\partial t}\,\mathrm{d}K_1(\tau,t)=-2\pi i\sum_{\substack{j=1\\ j\neq k}}^{N}\left\{\frac{\alpha_j}{R_j}\left[\sum_{m=2}^{M_{1j}}B_{-mj}(m-1)F_{mj}(t)-\sum_{m=0}^{M_{2j}}B_{mj}(m+1)F_{2k}(t)\overline{F_{(m+2)j}(t)}\right]\right.$$
$$\left.+\frac{\beta_j}{R_j}\left[\sum_{m=1}^{M_{2j}}\overline{B}_{mj}(m-1)F_{mj}(t)-\sum_{m=0}^{M_{1j}}\overline{B}_{-mj}(m+1)F_{2k}(t)\overline{F_{(m+2)j}(t)}\right]\right\}$$
$$\sum_{j=1}^{N}\int_{L_j}\overline{\Delta u_j(\tau)}\frac{\partial}{\partial t}\,\mathrm{d}K_2(\tau,t)=2\pi i\frac{\alpha_k+\beta_k}{R_k}B_{0k}-2\pi i\sum_{\substack{j=1\\ j\neq k}}^{N}\left\{\frac{\alpha_j}{R_j}\sum_{m=2}^{M_{1j}}\overline{B}_{-mj}(m-1)\overline{F_{mj}(t)}\Lambda(t)\right.$$
$$\left.-B_{0j}\frac{\alpha_j+\beta_j}{R_j}F_{2k}(t)\overline{F_{2j}(t)}+\frac{\beta_j}{R_j}\sum_{m=1}^{M_{2j}}B_{mj}(m-1)\overline{F_{mj}(t)}\Lambda(t)\right\} \tag{18}$$

4.3. Resulting equation

Substitution of expressions (17) and (18) into Eq. (4) results in the following equation:

$$-\sum_{m=2}^{M_{1k}}B_{-mk}\left(\frac{c_{1k}}{2}+\frac{m-1}{R_k}\alpha_k\right)F_{mk}(t)+\sum_{m=1}^{M_{2k}}B_{mk}\left(\frac{c_{3k}}{2}-\frac{m+1}{R_k}\alpha_k\right)\Big/F_{mk}(t)+\left(\frac{c_{2k}}{2}-2\frac{\alpha_k+\beta_k}{R_k}\right)B_{0k}$$
$$-\frac{\beta_k}{R_k}\left[\sum_{m=1}^{M_{2k}}\overline{B}_{mk}(m-1)F_{mk}(t)+\sum_{m=2}^{M_{1k}}\overline{B}_{-mk}(m+1)/F_{mk}(t)\right]+\sum_{\substack{j=1\\ j\neq k}}^{N}\left\{-\sum_{m=2}^{M_{1j}}B_{-mj}F_{mj}(t)\left(a_{1j}+\frac{m-1}{R_j}\alpha_j\right)\right.$$
$$+B_{0j}F_{2k}(t)\overline{F_{2j}(t)}\left(2a_{1j}-a_{3j}-2\frac{\alpha_j+\beta_j}{R_j}\right)+\sum_{m=1}^{M_{2j}}B_{mj}\overline{F_{mj}(t)}\left[\left(a_{1j}-a_{3j}-\frac{m+1}{R_j}\alpha_j\right)\right.$$
$$\left.\times F_{2k}(t)\overline{F_{2j}(t)}+(m-1)\frac{\beta_j}{R_j}\Lambda(t)\right]+\sum_{m=2}^{M_{1j}}\overline{B}_{-mj}\overline{F_{mj}(t)}\left[\left(a_{1j}+\frac{m-1}{R_j}\alpha_j\right)\Lambda(t)-(m+1)\frac{\beta_j}{R_j}F_{2k}(t)\overline{F_{2j}(t)}\right]$$
$$\left.-\frac{\beta_j}{R_j}\sum_{m=1}^{M_{2j}}\overline{B}_{mj}(m-1)F_{mj}(t)\right\}=-\frac{\kappa+1}{4\mu}\left[\sigma_{xx}^{\infty}+\sigma_{yy}^{\infty}-F_{2k}(t)\left(\sigma_{yy}^{\infty}-\sigma_{xx}^{\infty}-2i\sigma_{xy}^{\infty}\right)\right] \tag{19}$$

where

$$c_{1k}=2a_{1k}+a_{2k}-a_{3k};\qquad c_{2k}=4a_{1k}-a_{2k}-a_{3k};\qquad c_{3k}=2a_{1k}-a_{2k}-a_{3k}$$

By writing this equation for all the inclusions, $k=1$ to N, one gets a system of N complex algebraic equations. These equations involve $\sum_{k=1}^{N}(M_{1k}+M_{2k}-1)$ complex coefficients B_{-mk} $(m=2,\ldots,M_{1k})$ and B_{mk} $(m=1,\ldots,M_{2k})$, and N real coefficients B_{0k}.

4.4. Expressions for the potentials

Kolosov–Muskhelishvili potentials $\varphi(z)$ and $\psi(z)$ can be obtained by substituting (11) and (16) into (9). Again, the integrals can all be calculated analytically. If the evaluation point is inside an inclusion (e.g. $z\in D_k$) the final expressions for the potentials are (we neglect terms that provide rigid body movement)

$$
\begin{aligned}
\varphi(z) &= \frac{2\mu_k}{\kappa_k+1}\left\{\sum_{m=1}^{M_{2k}} B_{mk}\left(\frac{a_{1k}}{m+1}-\frac{\alpha_k}{R_k}\right)R_k/F_{(m+1)k}(z) - \sum_{m=2}^{M_{1k}}\overline{B}_{-mk}\beta_k/F_{(m+1)k}(z)\right.\\
&\quad\left.+\sum_{\substack{j=1\\ j\neq k}}^{N}\left[\sum_{m=2}^{M_{1j}} B_{-mj}\left(\frac{a_{1j}}{m-1}+\frac{\alpha_j}{R_j}\right)R_jF_{(m-1)j}(z) + \sum_{m=2}^{M_{2j}}\overline{B}_{mj}\beta_jF_{(m-1)j}(z)\right]\right\} + \varphi^{\infty}(z)\\
\psi(z) &= -\frac{2\mu_k}{\kappa_k+1}\left\{\sum_{m=1}^{M_{2k}} B_{mk}\left[(R_kF_{1k}(z)+\bar{z}_k)\left(a_{1k}-\frac{m+1}{R_k}\alpha_k-\frac{\beta_k}{R_k}\right)+\frac{\beta_k}{R_k}\bar{z}_k\right]\Big/F_{mk}(z)\right.\\
&\quad\left.+\sum_{m=2}^{M_{1k}}\overline{B}_{-mk}\left[\frac{a_{3k}-a_{1k}}{m-1}R_k-\beta_k(m+1)\left(1+\frac{\bar{z}_k}{R_kF_{1k}(z)}\right)-\alpha_k\right]\Big/F_{(m-1)k}(z)\right\}\\
&\quad-\frac{2\mu_k}{\kappa_k+1}\sum_{\substack{j=1\\ j\neq k}}^{N}\left\{B_{0j}\left(a_{3j}-2a_{1j}+2\frac{\alpha_j+\beta_j}{R_j}\right)R_jF_{1j}(z)\right.\\
&\quad+\sum_{m=1}^{M_{2j}}\overline{B}_{mj}\left[\frac{a_{3j-}a_{1j}}{m+1}R_jF_{1j}(z)-(m-1)\frac{\beta_j}{R_j}(R_jF_{1j}(z)+\bar{z}_j)+\alpha_jF_{1j}(z)\right]F_{mj}(z)\\
&\quad\left.-\sum_{m=2}^{M_{1j}}B_{-mj}\left[(R_jF_{1j}(z)+\bar{z}_j)\left(a_{1j}+\frac{m-1}{R_j}\alpha_j-\frac{\beta_j}{R_j}\right)+\frac{\beta_j}{R_j}\bar{z}_j\right]F_{mj}(z)\right\}+\psi^{\infty}(z)
\end{aligned}
\tag{20}
$$

In the case that the evaluation point z is inside the matrix, the potentials are

$$
\begin{aligned}
\varphi(z) &= \frac{2\mu}{\kappa+1}\sum_{j=1}^{N}\left[\sum_{m=2}^{M_{1j}} B_{-mj}\left(\frac{a_{1j}}{m-1}+\frac{\alpha_j}{R_j}\right)R_jF_{(m-1)j}(z) + \sum_{m=2}^{M_{2j}}\overline{B}_{mj}\beta_jF_{(m-1)j}(z)\right] + \varphi^{\infty}(z)\\
\psi(z) &= -\frac{2\mu}{\kappa+1}\sum_{j=1}^{N}\left\{B_{0j}\left(a_{3j}-2a_{1j}+2\frac{\alpha_j+\beta_j}{R_j}\right)R_jF_{1j}(z)\right.\\
&\quad+\sum_{m=1}^{M_{2j}}\overline{B}_{mj}\left[\frac{a_{3j-}a_{1j}}{m+1}R_jF_{1j}(z)-(m-1)\frac{\beta_j}{R_j}(R_jF_{1j}(z)+\bar{z}_j)+\alpha_jF_{1j}(z)\right]F_{mj}(z)\\
&\quad\left.-\sum_{m=2}^{M_{1j}}B_{-mj}\left[(R_jF_{1j}(z)+\bar{z}_j)\left(a_{1j}+\frac{m-1}{R_j}\alpha_j-\frac{\beta_j}{R_j}\right)+\frac{\beta_j}{R_j}\bar{z}_j\right]F_{mj}(z)\right\}+\psi^{\infty}(z)
\end{aligned}
\tag{21}
$$

The displacements and stresses inside the inclusions and the matrix can be calculated by using formulae (8), (10), (20), (21). Thus, the expressions for the stresses inside the inclusions and the matrix are given in Appendix B.

5. One inclusion

In the particular case of a single inclusion with center z_k, Eq. (19) has the form

$$
\begin{aligned}
&-\sum_{m=2}^{M_{1k}}B_{-mk}\left(\frac{c_{1k}}{2}+\frac{m-1}{R_k}\alpha_k\right)F_{mk}(t)+\sum_{m=1}^{M_{2k}}B_{mk}\left(\frac{c_{3k}}{2}-\frac{m+1}{R_k}\alpha_k\right)\Big/F_{mk}(t)+\left(\frac{c_{2k}}{2}-2\frac{\alpha_k+\beta_k}{R_k}\right)B_{0k}\\
&-\frac{\beta_k}{R_k}\left[\sum_{m=1}^{M_{2k}}\overline{B}_{mk}(m-1)F_{mk}(t)+\sum_{m=2}^{M_{1k}}\overline{B}_{-mk}(m+1)/F_{mk}(t)\right]=-\frac{\kappa+1}{4\mu}\left[\sigma_{xx}^{\infty}+\sigma_{yy}^{\infty}-F_{2k}(t)(\sigma_{yy}^{\infty}-\sigma_{xx}^{\infty}-2i\sigma_{xy}^{\infty})\right]
\end{aligned}
\tag{22}
$$

Both sides of this equation represent a truncated complex Fourier series. They are equal if and only if the corresponding complex coefficients for terms of the same power are equal. As a result we get the following system of equations:

$$\begin{aligned}
&-B_{-mk}\left(\frac{c_{1k}}{2}+\frac{m-1}{R_k}\alpha_k\right)-\overline{B}_{mk}\frac{m-1}{R_k}\beta_k=\begin{cases}\frac{\kappa+1}{4\mu}(\sigma_{yy}^{\infty}-\sigma_{xx}^{\infty}-2i\sigma_{xy}^{\infty}), & m=2\\ 0, & m\neq 2\end{cases}\\
&\left(\frac{c_{2k}}{2}-2\frac{\alpha_k+\beta_k}{R_k}\right)B_{0k}=-\frac{\kappa+1}{4\mu}\left(\sigma_{xx}^{\infty}+\sigma_{yy}^{\infty}\right)\\
&\left(\frac{c_{3k}}{2}-\frac{m+1}{R_k}\alpha_k\right)B_{mk}-\overline{B}_{-mk}\frac{m+1}{R_k}\beta_k=0,\quad m>0
\end{aligned}\tag{23}$$

One can see from the first and third of expressions (23) that the coefficients B_{mk} and B_{-mk} are both involved in the same equation of the system. This means that the number of terms in the two summations in (11) and (16) must be equal, i.e. $M_{1k}=M_{2k}$. The solution of system (23) leads to the following expressions for the only nonzero coefficients B_{-2k}, B_{0k}, and B_{2k}

$$\begin{aligned}
B_{-2k}&=\frac{-(\kappa+1)(\sigma_{yy}^{\infty}-\sigma_{xx}^{\infty}-2i\sigma_{xy}^{\infty})(-c_{3k}+6\alpha_k/R_k)R_k^2/8\mu}{3(\alpha_k^2-\beta_k^2)+\alpha_k(3c_{1k}-c_{3k})R_k/2-c_{1k}c_{3k}R_k^2/4}\\
B_{0k}&=\frac{(\kappa+1)(\sigma_{xx}^{\infty}+\sigma_{yy}^{\infty})/8\mu}{(\alpha_k+\beta_k)/R_k-c_{2k}/4}\\
B_{2k}&=\frac{3\beta_k(\kappa+1)(\sigma_{yy}^{\infty}-\sigma_{xx}^{\infty}+2i\sigma_{xy}^{\infty})R_k/4\mu}{3(\alpha_k^2-\beta_k^2)+\alpha_k(3c_{1k}-c_{3k})R_k/2-c_{1k}c_{3k}R_k^2/4}
\end{aligned}\tag{24}$$

Thus, a three-term truncated Fourier series gives the exact solution for the case of an isolated circular inclusion with a homogeneously imperfect interface. This result agrees with solutions obtained by Ru (1998) and Bigoni et al. (1998) by different methods.

As in case of perfect bonding we write a *real* analog of (23). We introduce the vector of the unknowns as follows:

$$\mathbf{X}_k=\begin{bmatrix}\mathbf{SX}_1(k)\\ \mathbf{SX}_2(k)\\ \mathbf{SX}_3(k)\end{bmatrix}\tag{25}$$

where the subvectors $\mathbf{SX}_1$, $\mathbf{SX}_2$, and $\mathbf{SX}_3$ are defined as

$$\mathbf{SX}_1(k)=\begin{bmatrix}\mathrm{Re}B_{-M_{1k}k}\\ \mathrm{Im}B_{-M_{1k}k}\\ \vdots\\ \mathrm{Re}B_{-2k}\\ \mathrm{Im}B_{-2k}\end{bmatrix};\qquad \mathbf{SX}_2(k)=\begin{bmatrix}B_{0k}\\ \mathrm{Re}B_{1k}\\ \mathrm{Im}B_{1k}\end{bmatrix};\qquad \mathbf{SX}_3(k)=\begin{bmatrix}\mathrm{Re}B_{2k}\\ \mathrm{Im}B_{2k}\\ \vdots\\ \mathrm{Re}B_{M_{1k}k}\\ \mathrm{Im}B_{M_{1k}k}\end{bmatrix}\tag{26}$$

Then a real system can be written in matrix form as

$$\mathbf{A}_{kk}\mathbf{X}_k=\mathbf{D}_k$$

where the vector of the right-hand side $\mathbf{D}_k$ has the form

$$\mathbf{D}_k=\begin{bmatrix}\mathbf{SD}_1\\ \mathbf{SD}_2\\ \mathbf{SD}_3\end{bmatrix}\tag{27}$$

and the only nonzero subvector $\mathbf{SD}_2$ is as follows:

$$\mathbf{SD}_2 = \begin{bmatrix} \frac{\kappa+1}{4\mu}(\sigma_{yy}^{\infty} - \sigma_{xx}^{\infty}) \\ -\frac{\kappa+1}{2\mu}\sigma_{xy}^{\infty} \\ -\frac{\kappa+1}{4\mu}(\sigma_{xx}^{\infty} + \sigma_{yy}^{\infty}) \end{bmatrix}$$

The square matrix $\mathbf{A}_{kk}$ of dimension $(n_k \times n_k)$ with

$$n_k = 4M_{1k} - 1 \tag{28}$$

can be written as

$$\mathbf{A}_{kk} = \begin{bmatrix} \mathbf{S}_{11}(k) & 0 & \mathbf{S}_{13}(k) \\ 0 & \mathbf{S}_{22}(k) & 0 \\ \mathbf{S}_{31}(k) & 0 & \mathbf{S}_{33}(k) \end{bmatrix} \tag{29}$$

where four square submatrices $\mathbf{S}_{11}(k)$, $\mathbf{S}_{13}(k)$, $\mathbf{S}_{31}(k)$, and $\mathbf{S}_{33}(k)$ have the dimension $2M_{1k} - 2 \times 2M_{1k} - 2$ and the submatrix $\mathbf{S}_{22}(k)$ has the dimension 3×3. These submatrices can be written as follows:

$$\mathbf{S}_{11}(k) = -\begin{bmatrix} \frac{c_{1k}}{2} + \frac{(M_{1k}-1)\alpha_k}{R_k} & 0 & 0 & 0 & 0 \\ 0 & \frac{c_{1k}}{2} + \frac{(M_{1k}-1)\alpha_k}{R_k} & 0 & 0 & 0 \\ 0 & 0 & \ddots & 0 & 0 \\ 0 & 0 & 0 & \frac{c_{1k}}{2} + \frac{\alpha_k}{R_k} & 0 \\ 0 & 0 & 0 & 0 & \frac{c_{1k}}{2} + \frac{\alpha_k}{R_k} \end{bmatrix} \tag{30}$$

$$\mathbf{S}_{13}(k) = \begin{bmatrix} -\frac{\beta_k}{R_k} & 0 & 0 & 0 & 0 \\ 0 & \frac{\beta_k}{R_k} & 0 & 0 & 0 \\ 0 & 0 & \ddots & 0 & 0 \\ 0 & 0 & 0 & -\frac{(M_{1k}-1)\beta_k}{R_k} & 0 \\ 0 & 0 & 0 & 0 & \frac{(M_{1k}-1)\beta_k}{R_k} \end{bmatrix} \tag{31}$$

$$\mathbf{S}_{31}(k) = \begin{bmatrix} -\frac{(M_{1k}+1)\beta_k}{R_k} & 0 & 0 & 0 & 0 \\ 0 & \frac{(M_{1k}+1)\beta_k}{R_k} & 0 & 0 & 0 \\ 0 & 0 & \ddots & 0 & 0 \\ 0 & 0 & 0 & -\frac{3\beta_k}{R_k} & 0 \\ 0 & 0 & 0 & 0 & \frac{3\beta_k}{R_k} \end{bmatrix} \tag{32}$$

$$\mathbf{S}_{33}(k) = \begin{bmatrix} \frac{c_{3k}}{2} - \frac{3\alpha_k}{R_k} & 0 & 0 & 0 & 0 \\ 0 & \frac{c_{3k}}{2} - \frac{3\alpha_k}{R_k} & 0 & 0 & 0 \\ 0 & 0 & \ddots & 0 & 0 \\ 0 & 0 & 0 & \frac{c_{3k}}{2} - \frac{(1+M_{1k})\alpha_k}{R_k} & 0 \\ 0 & 0 & 0 & 0 & \frac{c_{3k}}{2} - \frac{(1+M_{1k})\alpha_k}{R_k} \end{bmatrix} \tag{33}$$

$$\mathbf{S}_{22}(k)=\begin{bmatrix}\frac{c_{2k}}{2}-2\frac{\alpha_k+\beta_k}{R_k} & 0 & 0\\ 0 & \frac{c_{3k}}{2}-\frac{2\alpha_k}{R_k} & 0\\ 0 & 0 & \frac{c_{3k}}{2}-\frac{2\alpha_k}{R_k}\end{bmatrix}$$

The matrix $\mathbf{A}_{kk}$ can be inverted analytically. The resulting matrix $\mathbf{A}_{kk}^{-1}$ is as follows:

$$\mathbf{A}_{kk}^{-1}=\begin{bmatrix}\left(\mathbf{S}_{11}-\mathbf{S}_{13}\mathbf{S}_{33}^{-1}\mathbf{S}_{31}\right)^{-1} & 0 & -\mathbf{S}_{11}^{-1}\mathbf{S}_{13}\left(\mathbf{S}_{33}-\mathbf{S}_{31}\mathbf{S}_{11}^{-1}\mathbf{S}_{13}\right)^{-1}\\ 0 & \mathbf{S}_{22}^{-1} & 0\\ -\mathbf{S}_{33}^{-1}\mathbf{S}_{31}\left(\mathbf{S}_{11}-\mathbf{S}_{13}\mathbf{S}_{33}^{-1}\mathbf{S}_{31}\right)^{-1} & 0 & \left(\mathbf{S}_{33}-\mathbf{S}_{31}\mathbf{S}_{11}^{-1}\mathbf{S}_{13}\right)^{-1}\end{bmatrix} \tag{34}$$

where the argument k in $\mathbf{S}_{11}$, etc. is omitted for brevity.

Because of the simple diagonal form of the submatrices $\mathbf{S}$, the calculations in (34) are trivial. This allows one to save computational time, which is an important issue in solving large-scale problems.

6. *N* inclusions

In the general case of N inclusions we have a system of N complex algebraic equations of the type (19) for $t\in L_k$, $k=1,\ldots,N$. As in Mogilevskaya and Crouch (2001) we use the Galerkin method (e.g. Brebbia et al., 1984) to get a linear algebraic system.

Consider again the case when $t\in L_k$. We successively multiply both sides of Eq. (19) by the powers $(t-z_k)^l$ $[l=-(M_{1k}+1),-M_{1k},\ldots,-1,1,2,\ldots,M_{1k}-1]$ and integrate over L_k, noting that we now require $M_{2k}=M_{1k}$. The integrations can again be done analytically by using the three basic integrals from Appendix A (see Mogilevskaya and Crouch, 2001, for details of analogous calculations for the case of perfect bonding). This gives the following system of equations with respect to the unknowns B_{-mj} and B_{mj}:

(i) $M_{1k}-1$ equations ($l=1,\ldots,M_{1k}-1$)

$$\begin{aligned}&-\left(\frac{c_{1k}}{2}+l\frac{\alpha_k}{R_k}\right)B_{-(l+1)k}-l\frac{\beta_k}{R_k}\overline{B}_{(l+1)k}+\sum_{\substack{j=1\\ j\neq k}}^{N}\overline{F_{(l-1)k}(z_j)}\left\{\left(2a_{1j}-a_{3j}-2\frac{\alpha_j+\beta_j}{R_j}\right)l\overline{F_{2j}(z_k)}B_{0j}.\right.\\ &\quad+\sum_{m=2}^{M_{1j}}l\binom{m+l-1}{m-1}\overline{B}_{-mj}\overline{F_{mj}(z_k)}\left[\left(\overline{F_{2k}(z_j)}\frac{m+l}{l+1}+\overline{F_{2j}(z_k)}\frac{m+l}{m}-\frac{z_k-z_j}{\overline{z}_k-\overline{z}_j}\right)\left(a_{1j}+\frac{m-1}{R_j}\alpha_j\right)\right.\\ &\quad\left.-\frac{\beta_j}{R_j}\frac{m+l}{m}\overline{F_{2j}(z_k)}\right]+\sum_{m=1}^{M_{1j}}\binom{m+l}{m+1}B_{mj}\overline{F_{(m+2)j}(z_k)}\\ &\quad\times\left[a_{1j}-a_{3j}-\frac{m+1}{R_j}\alpha_j+\frac{(m+1)(m-1)}{R_j}\beta_j\left(1+\frac{m}{l+1}\frac{R_k^2}{R_j^2}-\frac{m}{m+l}\frac{\left(z_k-z_j\right)\left(\overline{z}_k-\overline{z}_j\right)}{R_j^2}\right)\right]\Bigg\}\\ &=\begin{cases}\frac{\kappa+1}{4\mu}(\sigma_{yy}^{\infty}-\sigma_{xx}^{\infty}-2i\sigma_{xy}^{\infty}), & l=1\\ 0, & l\neq 1\end{cases}\end{aligned} \tag{35}$$

(ii) the equation

$$\left(\frac{c_{2k}}{2}-2\frac{\alpha_k+\beta_k}{R_k}\right)B_{0k}-\sum_{\substack{j=1\\ j\neq k}}^{N}\left\{\sum_{m=2}^{M_{1j}}\left(a_{1j}+\frac{m-1}{R_j}\alpha_j\right)\left[B_{-mj}F_{mj}(z_k)+\overline{B}_{-mj}\overline{F_{mj}(z_k)}\right]\right.$$
$$\left.+\frac{\beta_j}{R_j}\sum_{m=1}^{M_{1j}}(m-1)\left[B_{mj}\overline{F_{mj}(z_k)}+\overline{B}_{mj}F_{mj}(z_k)\right]\right\}=-\frac{\kappa+1}{4\mu}\left(\sigma_{xx}^{\infty}+\sigma_{yy}^{\infty}\right) \tag{36}$$

(iii) M_{1k} equations ($l=2,\ldots,M_{1k}+1$)

$$\left(\frac{c_{3k}}{2}-l\frac{\alpha_k}{R_k}\right)B_{(l-1)k}-l\frac{\beta_k}{R_k}\overline{B}_{-(l-1)k}-\sum_{\substack{j=1\\ j\neq k}}^{N}F_{(l-1)k}(z_j)\sum_{m=2}^{M_{1j}}\left(a_{1j}+\frac{m-1}{R_j}\alpha_j\right)\binom{m+l-2}{m-1}B_{-mj}F_{mj}(z_k)=0 \tag{37}$$

where the binomial coefficients are defined as

$$\binom{n}{k}=\frac{n!}{k!(n-k)!} \tag{38}$$

By writing these equations for $k=1,\ldots,N$ and separating real and imaginary parts, we get finally the real system of $\sum_{k=1}^{N}n_k$ (where n_k is given by (28)) linear algebraic equations

$$\mathbf{AX}=\mathbf{D} \tag{39}$$

The matrix of this system has the following form

$$\mathbf{A}=\begin{bmatrix}\mathbf{A}_{11} & \cdots & \mathbf{A}_{1N}\\ \vdots & \vdots & \vdots\\ \mathbf{A}_{N1} & \cdots & \mathbf{A}_{NN}\end{bmatrix} \tag{40}$$

where $\mathbf{A}_{kk}$ is submatrix (29) corresponding to the case of an isolated kth inclusion. The submatrix $\mathbf{A}_{kj}$ ($j\neq k$) of dimension $(n_k\times n_j)$ is a full submatrix that expresses the influence of the jth inclusion on the kth inclusion. The individual terms of this matrix are functions of the distances between the centers of the kth and jth inclusions, as well as their interface parameters and radii. The vector of unknowns $\mathbf{X}$ and the right-hand side vector $\mathbf{D}$ can be written as

$$\mathbf{X}=\begin{bmatrix}\mathbf{X}_1\\ \vdots\\ \mathbf{X}_N\end{bmatrix};\qquad \mathbf{D}=\begin{bmatrix}\mathbf{D}_1\\ \vdots\\ \mathbf{D}_N\end{bmatrix}$$

where subvectors $\mathbf{X}_k$ and $\mathbf{D}_k$ are given by formulae (25) and (27).

The system (39) can be solved by using a Gauss–Seidel iterative algorithm (Golub and Van Loan, 1996). In this algorithm the new iteration $\mathbf{X}^{(k+1)}$

$$\mathbf{X}^{(k+1)}=\begin{bmatrix}\mathbf{X}_1^{(k+1)}\\ \vdots\\ \mathbf{X}_N^{(k+1)}\end{bmatrix}$$

can be obtained as follows:

$$\mathbf{X}_l^{(k+1)}=\mathbf{A}_{ll}^{-1}\left[\mathbf{D}_l-\sum_{j=1}^{l-1}\mathbf{A}_{lj}\mathbf{X}_j^{(k+1)}-\sum_{j=l+1}^{N}\mathbf{A}_{lj}\mathbf{X}_j^{(k)}\right],\quad l=1,\ldots,N \tag{41}$$

The iteration process is deemed to have converged when the maximum difference between two successive iterates reaches a predetermined tolerance limit for each $\mathbf{X}_l$.

As in case of perfect bonding, there is no need to store the full matrix (40) in computer memory for the solution of (39), and the diagonal matrix $\mathbf{A}_{ll}$ is trivial to invert. The number of terms M_{1j} of the complex Fourier series can be determined during the iterative procedure as explained by Mogilevskaya and Crouch (2001).

7. Artificial inclusion

The case of an "artificial inclusion" provides the simplest benchmark for the algorithm given above. Consider two elastic inclusions, one with boundary L_1, center $z_1 = 0$, radius R_1, and elastic constants μ_1 and ν_1, which are different from those of the matrix (μ and ν), and the other with boundary L_2, center z_2, radius R_2, and elastic constants $\mu_2 = \mu$ and $\nu_2 = \nu$. The bond between the first inclusion and the matrix is assumed to be homogeneously imperfect; the second inclusion is perfectly bonded to the matrix. The solution for a single inclusion can then be used to calculate the elastic fields everywhere in the plane. In particular, we can calculate the tractions on the boundary of the artificial inclusion. The expression for the tractions has the following form (Muskhelishvili, 1959):

$$\sigma_2(\tau) = \Phi(\tau) + \overline{\Phi(\tau)} - \exp(-2i\theta_2)\left[\tau\overline{\Phi'(\tau)} + \overline{\Psi(\tau)}\right] \tag{42}$$

where $\tau \in L_2$; $\Phi(\tau) = \varphi'(\tau)$; $\Psi(\tau) = \psi'(\tau)$ and θ_2 is the polar angle at the point τ.

By using expressions (21) for the potentials and solution (24) for the coefficients, one can write the potentials $\Phi(z)$ and $\Psi(z)$ at any point z outside the "real" inclusion as

$$\begin{aligned} \Phi(z) &= C_1 - \frac{C_2}{z^2} \\ \Psi(z) &= C_3 + 2\frac{C_1 - C_4}{z^2}R_1^2 - 3R_1^2\frac{C_2 + \overline{C}R_1^4}{z^4} \end{aligned} \tag{43}$$

where the coefficients C_l $(l = 1, \ldots, 5)$ can be expressed via those from (24) as

$$C_1 = \frac{\sigma_{xx}^{\infty} + \sigma_{yy}^{\infty}}{4}; \qquad C_3 = \frac{\sigma_{yy}^{\infty} - \sigma_{xx}^{\infty} + 2i\sigma_{xy}^{\infty}}{2}; \qquad C_2 = -R_1^2(\overline{C}_3 + B_{-21}); \qquad C_4 = \frac{B_{01}}{2}; \qquad C_5 = \frac{B_{21}}{3R_1^2}$$

By substituting expressions (43) into Eq. (42) and performing some algebra, one gets the following expression for the tractions σ_2 on the boundary L_2:

$$\sigma_2(\tau) = 2C_1 - \frac{C_2}{\tau^2} - \frac{\overline{C}_2}{\bar{\tau}^2} - \frac{R_2^2}{(\tau - z_2)^2}\left[2\tau\frac{\overline{C}_2}{\bar{\tau}^3} + \overline{C}_3 + 2\frac{C_1 - C_4}{\bar{\tau}^2}R_1^2 - 3R_1^2\frac{\overline{C}_2 + C_5R_1^4}{\bar{\tau}^4}\right], \quad \tau \in L_2 \tag{44}$$

Taking into account that

$$\tau = (\tau - z_2) + z_2 = z_2\left(1 + \frac{\tau - z_2}{z_2}\right), \quad \left|\frac{\tau - z_2}{z_2}\right| < 1$$
$$(\bar{\tau} - \bar{z}_2)(\tau - z_2) = R_2^2$$

and using the series expansion

$$(1+z)^m = 1 + \frac{m}{1!}z + \frac{m(m-1)}{2!}z^2 + \cdots + \frac{m(m-1)\cdots(m-n+1)}{n!}z^n + \cdots, \quad |z| < 1$$

all of the terms involved in (44) can be decomposed into a series with respect to $\tau - z_2$. In this way, σ_2 can finally be written as

$$\sigma_2(\tau) = \sum_{m=1}^{\infty} B_{-m2} F_{m2} + \sum_{m=0}^{\infty} B_{m2}/F_{m2} \tag{45}$$

where

$$\begin{aligned}
B_{02} &= 2C_1 - \frac{C_2}{z_2^2} - \frac{\overline{C}_2}{\overline{z}_2^2} \\
B_{-22} &= -\overline{C}_3 + 3\frac{\overline{C}_2 R_2^2}{\overline{z}_2^4} - 2(C_1 - C_4)\frac{R_1^2}{\overline{z}_2^2} - 2\overline{C}_2 \frac{z_2}{\overline{z}_2^3} + 3R_1^2 \frac{\overline{C}_2 + C_5 R_1^4}{\overline{z}_2^4} \\
B_{-m2} &= (-1)^m (m-1)\frac{R_2^m}{\overline{z}_2^m}\left[(m+1)\frac{\overline{C}_2}{\overline{z}_2^2} - m\frac{\overline{C}_2}{R_2^2}\frac{z_2}{\overline{z}_2} - 2(C_1 - C_4)\frac{R_1^2}{R_2^2} + m(m+1)\frac{R_1^2}{2R_2^2}\frac{\overline{C}_2 + C_5 R_1^4}{\overline{z}_2^2}\right], \quad m \geqslant 3 \\
B_{m2} &= (-1)^{m+1}(m+1) C_2 \frac{R_2^m}{z_2^{m+2}}, \quad m \geqslant 1
\end{aligned} \tag{46}$$

8. Numerical examples

8.1. Artificial inclusion

Representation (45) gives the analytic solution for the case of an artificial inclusion. This solution provides an opportunity to conduct numerical experiments to check the numerical algorithm (41) and determine how many terms of the complex Fourier series are needed to achieve a predetermined accuracy level.

Consider the case of biaxial tension at infinity ($\sigma_{xx}^{\infty} = \sigma_{yy}^{\infty} = 1$). Suppose that the first inclusion has center $z_1 = (0,0)$, radius $R_1 = 2$, and elastic constants $\mu_1 = 1$ and $\nu_1 = 0.2$. The elastic constants for the matrix are equal to $\mu = 0.5$ and $\nu = 0.25$. The second inclusion is perfectly bonded and has the same elastic constants as the matrix. Consider the following cases for the location and size of the artificial inclusion: (i) $z_2 = (8,0)$, $R_2 = 1$; (ii) $z_2 = (4,0)$, $R_2 = 1$; (iii) $z_2 = (3.1,0)$, $R_2 = 1$. The interfacial parameters for the first inclusion were chosen as follows: (a) $\lambda_{jn} = 0$, $\lambda_{js} = 1$; (b) $\lambda_{jn} = 1$, $\lambda_{js} = 0$; (c) $\lambda_{jn} = 1$, $\lambda_{js} = 1$; (d) $\lambda_{jn} = 0$, $\lambda_{js} = 10$; (e) $\lambda_{jn} = 10$, $\lambda_{js} = 0$; and (f) $\lambda_{jn} = 10$, $\lambda_{js} = 10$.

In all these cases the tractions $\sigma_2(\tau)$ were calculated both analytically by using formulae (45) and (46) and numerically by using the Gauss–Seidel algorithm (41). The parameters δ_1 and δ_2 were chosen as $\delta_1 = 10^{-4}\min\{B_{01}, B_{02}\}$ and $\delta_2 = 0.01$. All calculations were performed on a personal computer using single precision arithmetic. Three coefficients B_{-21}, B_{01}, and B_{21} (24) provided the analytical solution for the first inclusion, and the numerical results for these coefficients coincided with the analytical solution to seven significant digits.

For case (i) with interfacial parameters (a), (b), (c), and (d), convergence within the specified accuracy was achieved with two only nonzero coefficients B_{-22} and B_{02}. For interfacial parameters (e) and (f) three nonzero coefficients B_{-32}, B_{-22}, and B_{02} were needed. In all of these cases the Gauss–Seidel algorithm converged within two or three iterations for each step (with the chosen fixed number of terms). The values of the coefficients coincided with the analytical solution to seven significant digits.

When the inclusions are closer to each other, more terms are needed to achieve a predetermined accuracy level. For case (ii) with interfacial parameters (a), (b), (c), and (d), four nonzero coefficients B_{-m2}

($m = 0, 2, \ldots, 4$) were needed. For interfacial parameters (e) and (f), seven nonzero coefficients B_{-m2} ($m = 0, 2, \ldots, 7$) were needed.

For case (iii) with interfacial parameters (a), (b), (c), and (d), the number of nonzero coefficients B_{-m2} was equal to five ($m = 0, 2, \ldots, 5$). For interfacial parameters (e) and (f), seven nonzero coefficients B_{-m2} ($m = 0, 2, \ldots, 7$) were needed.

The accuracy in calculation of the coefficients B_{-m2} was excellent for all of these cases (the same as in case (i)). A Gauss–Seidel algorithm converged for all the cases within three iterations for each step (with the chosen fixed number of terms).

A case when the artificial inclusion is larger than the real one requires more terms of the complex Fourier series to achieve a predetermined accuracy level. For example, consider a case when $z_1 = (0, 0)$, $R_1 = 0.5$ and $z_2 = (2, 0)$, $R_2 = 1$. The number of nonzero coefficients B_{-m2} was equal to five for conditions (a) and (d); seven for conditions (b) and (c), and eight for conditions (e) and (f).

8.2. Equally spaced inclusions

As a more comprehensive example, we consider the *finite* rectangular $l \times l$ array (l in each coordinate direction) of inclusions shown in Fig. 2. All inclusions have the same radii a and elastic properties $\mu_i = 5.5 \times 10^3$ MPa and $\nu_i = 0.25$. The elastic properties of the matrix were taken as $\mu_m = 0.7 \times 10^3$ MPa and $\nu_m = 0.33$. The dimensionless interfacial constants were equal to $\lambda_{jn}/(\mu_m/a) = \lambda_{js}/(\mu_m/a) = \lambda = 0$, 0.1, and 1.0. The distances between the centers of the fibers in the x- and y-directions were uniform and equal to $2b$ and $b/a = \sqrt{\pi/2}$, respectively. We studied the stress and traction distribution in the basic cell ($0 \leqslant x \leqslant b$, $0 \leqslant y \leqslant b$). We took $l = 5$, 7, 9, and 11 with parameters δ_1 and δ_2 chosen as $\delta_1 = 10^{-4} \min\{B_{01}, B_{02}, \ldots, B_{0l}\}$, and $\delta_2 = 0.01$. Convergence within the specified accuracy was achieved with up to a total of 17 coefficients B_{-mj} and B_{mj}. The distributions of tractions and stresses in the basic cell were the same for all values of l considered. To avoid radial overlap we consider the case of pure sliding with $\lambda_{jn}/(\mu_m/a) = 0$, $\lambda_{js}/(\mu_m/a) = \lambda = 0$, 0.1, and 1.0. (Prohibition of radial overlap would otherwise require an inhomogeneously imperfect interface, which is outside the scope of this paper.) Fig. 3 shows the interface stresses for the central inclusion as obtained by our approach.

For the case of perfect bonding ($\lambda = 0$) we performed additional calculations with the complex variables boundary element computer code described in Mogilevskaya (1996). This code allows the use of circular arc elements with the unknown tractions approximated by complex Lagrange polynomials of the second degree. Three collocation points for each element (the nodes of the Lagrange polynomials) were distributed uniformly along each element. The array of 25 circular inclusions was considered, and each inclusion was

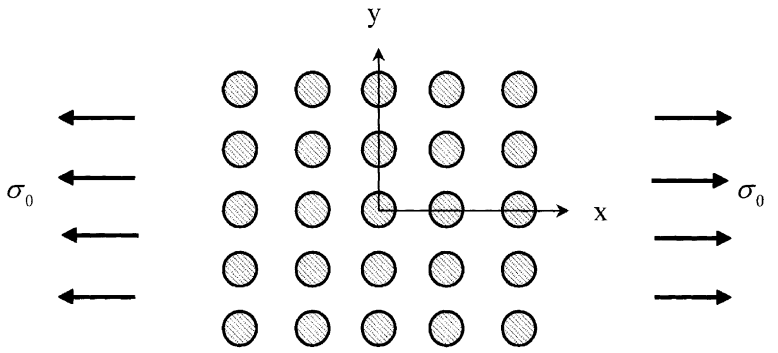

Fig. 2. Rectangular array of inclusions.

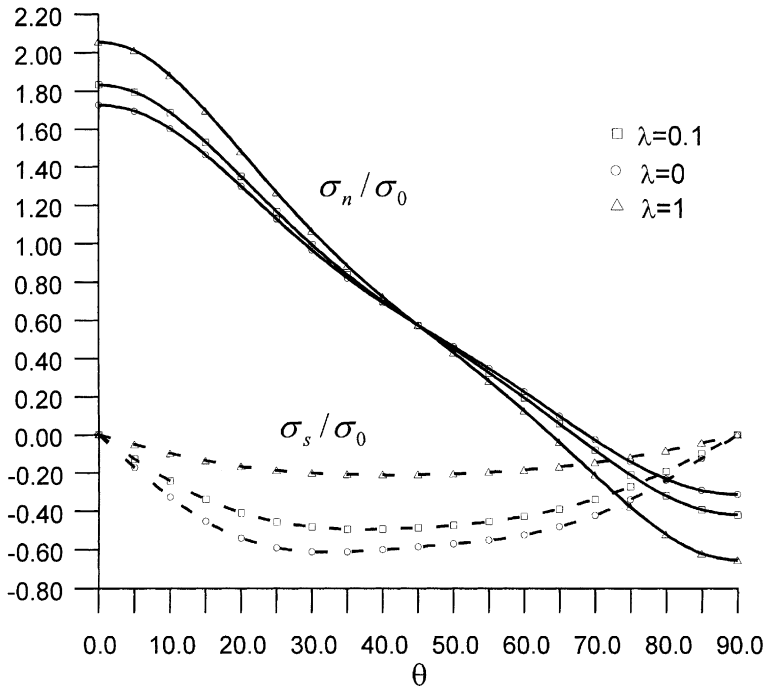

Fig. 3. Interface tractions for the central inclusion ($\lambda_n = 0$, $\lambda_s = \lambda$).

approximated by 4 and 8 circular elements, respectively. The results are shown in Fig. 4. One can see that the results with 8 circular elements correspond well to those obtained by the present approach. Additional validation of our results was obtained by using a real variables boundary integral analog (Crouch and Mogilevskaya, 2002) of the approach described herein.

The analogous problem for an *infinite* rectangular array was solved by Achenbach and Zhu (1989), who reduced the problem to a boundary integral equation written for a quarter region of a basic cell. (This was possible because of the periodicity of the fibers in the composite.) In case unrealistic radial overlap of the two materials occurred over a part of the interface, Achenbach and Zhu repeated all the calculations assuming that the displacements were continuous on that part of the boundary. For the case of perfect bonding ($\lambda = 0$) we compared our results with those of Achenbach and Zhu (1989) (Fig. 4). One can see that the difference between the two sets of results increases as $\theta \to 0°$ and $\theta \to 90°$.

The reason for this difference lies in the different physical nature of two problems. The finite array of inclusions in effect behaves as an inclusion with some average properties embedded in a matrix with different elastic properties, whereas the infinite array can be viewed as a homogeneous plane with average elastic properties. When the inclusions are relatively far apart, the two solutions are comparable, but otherwise are quite different.

Fig. 5 shows the comparison of results obtained by the different approaches for the internal stress σ_{xx} along the line $x = 0$, $0 \leqslant y \leqslant b$. The discrepancies between our results and the ones by Achenbach and Zhu are even more pronounced than for the interface tractions. The complex variables boundary element code gave good agreement with the present approach for a relatively fine mesh (16 elements for the central circle and 8 elsewhere).

Another example is concerned with the hexagonal arrays of periodically spaced inclusions. An example of such an array is shown in Fig. 6. The material properties for the inclusions and matrix were taken as

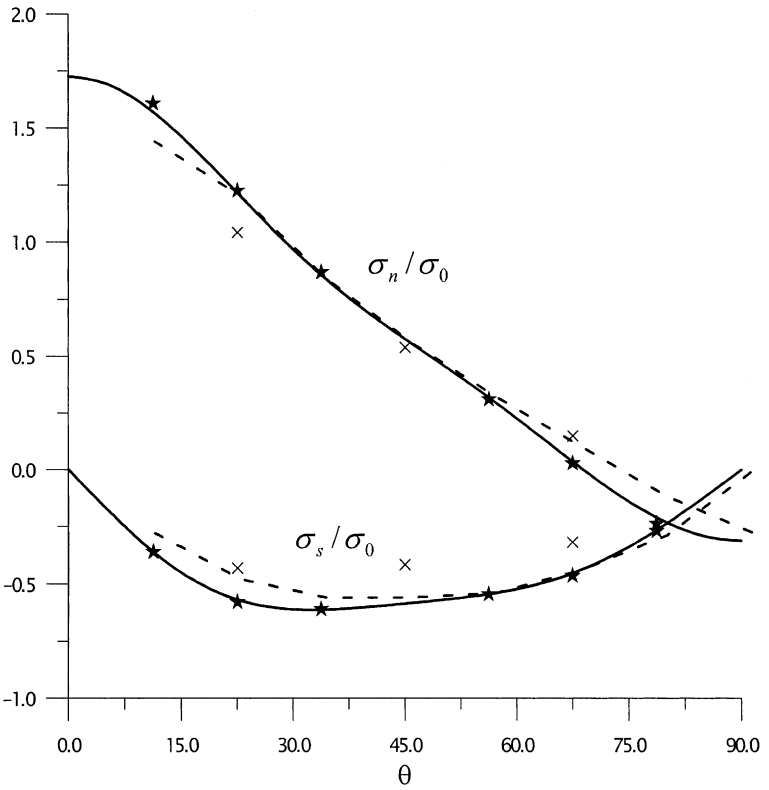

Fig. 4. Interface tractions for the central inclusion, perfect bond (solid line—present approach; dashed line—results from Achenbach and Zhu (1989); ×—BEM results with 4 elements; ★—BEM results with 8 elements).

$\mu_i = 30$ Msi, $\nu_i = 0.22$ and $\mu_m = 14.2$ Msi, $\nu_m = 0.22$. The ratio b/a was $\sqrt{5\pi/3\sqrt{3}}$ and the interfacial constants were taken as $\lambda_{jn}/(\mu_m/a) = \lambda_{js}/(\mu_m/a) = \lambda = 0$, 0.1, and 1.0. We calculated the case of a hexagonal array with 25 periodically spaced inclusions. The parameters δ_1 and δ_2 were chosen as in the previous example. Radial overlap does not occur when $\lambda = 0$ and $\lambda = 0.1$, and for these cases we compared the results with the ones for an infinite array given in Achenbach and Zhu (1990). The comparisons with results from Achenbach and Zhu (1990) and the complex variables boundary element code are shown in Figs. 7–10. In this case the volume content of the fibers ($c = 0.4$) was smaller than for the rectangular array ($c = 0.5$) and the agreement between our results and those by Achenbach and Zhu is better.

8.3. Calculation time

To investigate the dependence of the calculation time on the number of inclusions, we conducted numerical experiments with the hexagonal array of periodically spaced inclusions described in the previous subsection (the volume content of the fibers was $c = 0.4$). The parameters δ_1 and δ_2 were chosen as before, and the calculations were performed with an 866 MHz personal computer. Convergence within the specified accuracy was achieved with 15 coefficients B_{-mj} and B_{mj} for all cases considered. The dependence of the calculation time on the number of inclusions is shown in Fig. 11 for the case of perfect bonding. This case

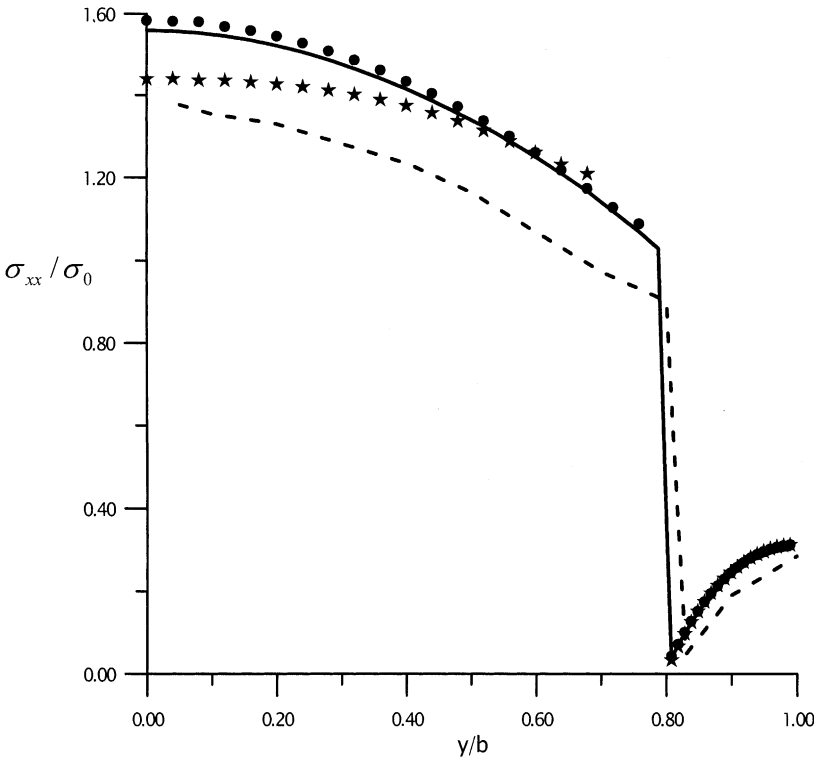

Fig. 5. Stress along line $x = 0$, $0 \leqslant y \leqslant b$ (solid line—present approach; dashed line—results from Achenbach and Zhu (1989); ★—BEM results with 8 elements; ●—BEM results with 16 elements).

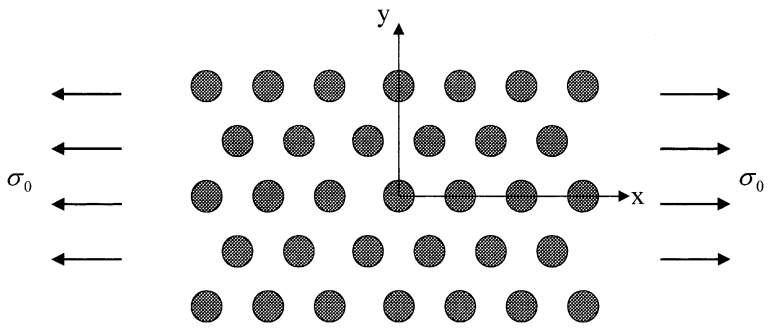

Fig. 6. Hexagonal array of inclusions.

was selected because it required more time than the analogous case with imperfect interfaces. The calculation times for this example could easily be reduced by taking into account that the interactions between inclusions decay rapidly with distance. Thus, fewer terms of the Fourier series are needed to accurately capture the interactions between inclusions that are far apart than those that are close together. Work is in progress to incorporate refinements of this sort into the equation-solving algorithm, and it is expected that substantial savings in computer run-times can be realized without a noticeable loss in accuracy.

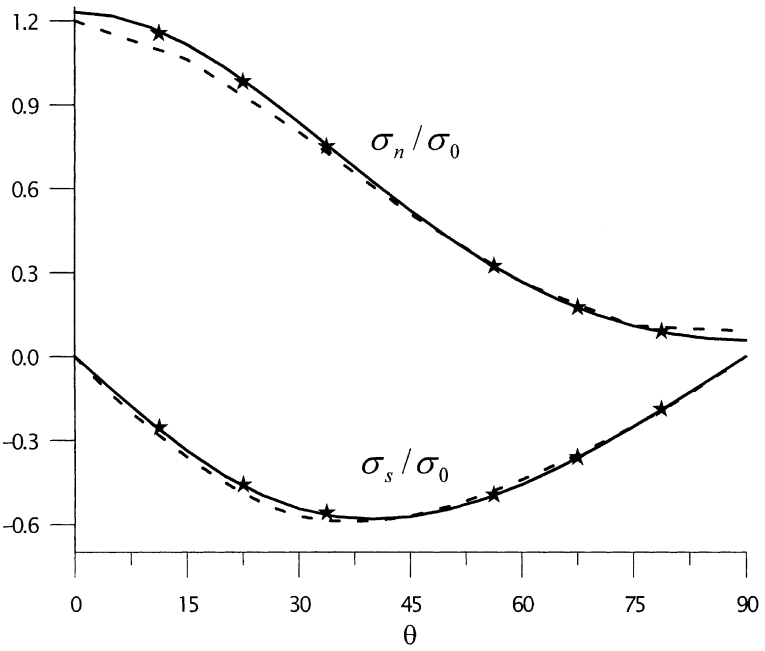

Fig. 7. Interface tractions for the central inclusion, perfect bond (solid line—present approach; dashed line—results from Achenbach and Zhu (1990); ★—BEM results with 8 elements).

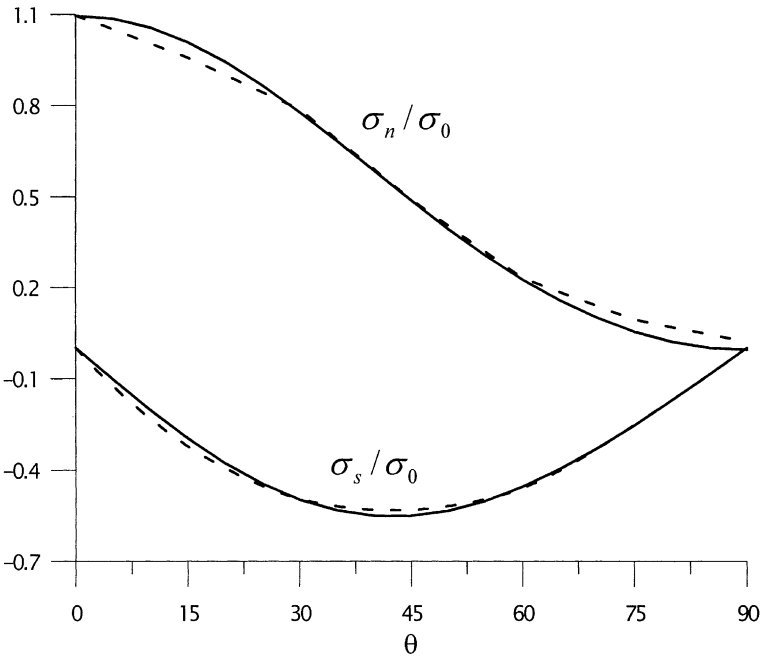

Fig. 8. Interface tractions for the central inclusion, $\lambda_{jn}/(\mu_m/a) = \lambda_{js}/(\mu_m/a) = 0.1$ (solid line—present approach; dashed line—results from Achenbach and Zhu, 1990).

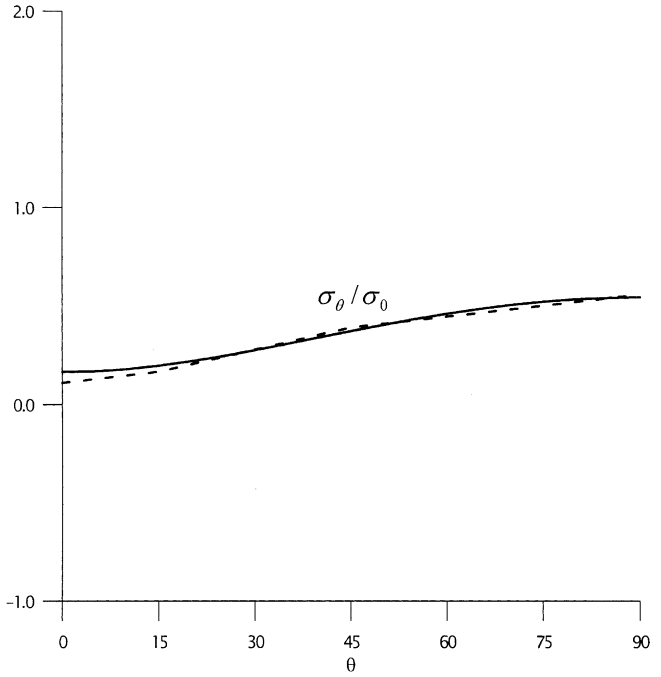

Fig. 9. Circumferential stress at the matrix side of the interface, perfect bond (solid line—present approach; dashed line—results from Achenbach and Zhu, 1990).

9. Conclusions

In this paper we extended a recently suggested numerical technique for solving the problem of an infinite elastic plane containing a large number of circular elastic inclusions to the case of inclusions with homogeneously imperfect interfaces. Comparison of the results with analytical and numerical solutions available in the literature has proven the effectiveness of the method and its potential in solving large-scale problems with large numbers of inclusions. Obvious future developments of the method are the implementation of finite boundaries, elliptical inclusions, and inhomogeneously imperfect interfaces. The work in progress on a real variables analog of the method will allow us to extend this approach to three-dimensional problems.

Appendix A. Three basic integrals ($m, n > 0$)

The detailed derivations of these integrals are given in Mogilevskaya and Crouch (2001).

$$I_1 = \int_{L_k} \frac{\mathrm{d}\tau}{(\tau - z)^m} = \begin{cases} 2\pi i & z \in D_k,\ m = 1 \\ 0 & z \in D_k,\ m > 1 \\ 0 & z \notin D_k \cup L_k \\ \pi i & z = t \in L_k,\ m = 1 \end{cases}$$

$$I_2 = \int_{L_k} \frac{\mathrm{d}\tau}{(\tau - z_k)^m (\tau - z)^n} = \begin{cases} 0 & z \in D_k \\ 2\pi i \binom{m+n-2}{n-1} \frac{(-1)^{m-1}}{(z_k - z)^{m+n-1}} & z \notin D_k \cup L_k \\ -\frac{\pi i}{(t - z_k)^m} & z \in L_k,\ n = 1 \end{cases}$$

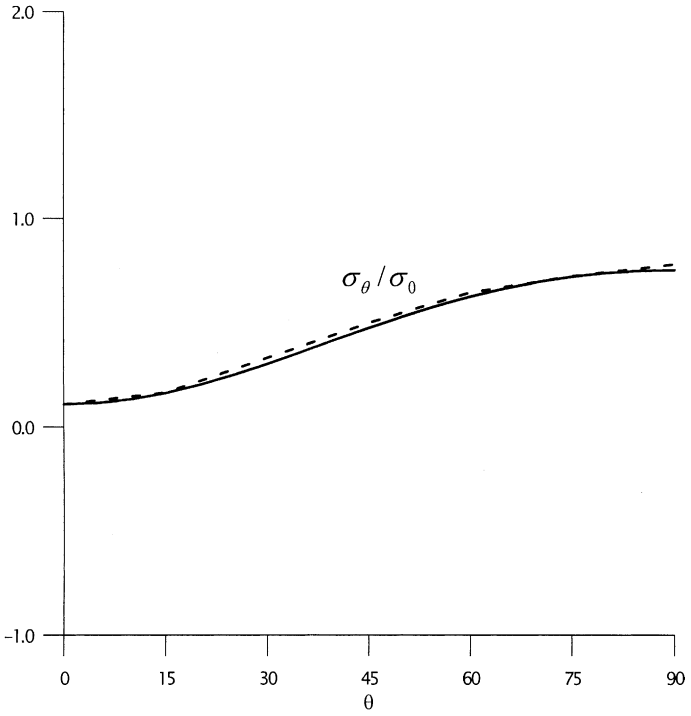

Fig. 10. Circumferential stress at the matrix side of the interface, $\lambda = 0.1$ (solid line—present approach; dashed line—results from Achenbach and Zhu, 1990).

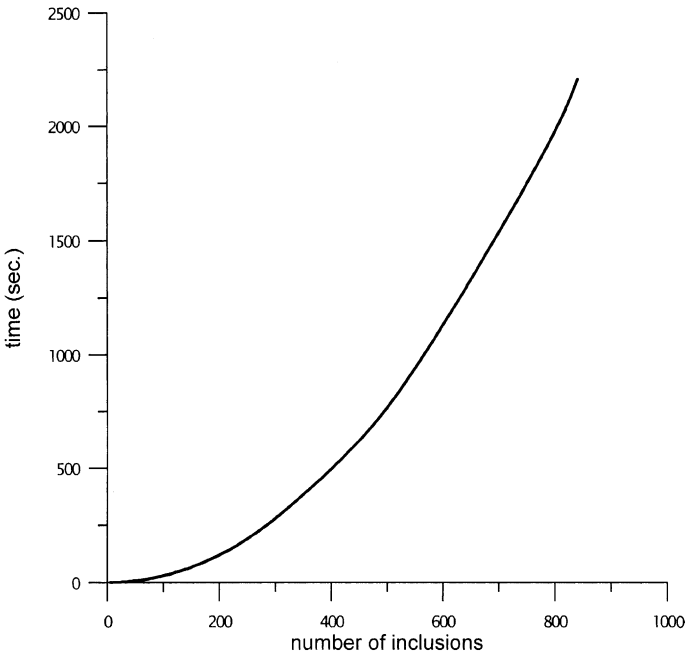

Fig. 11. Dependence of the calculation time on the number of inclusions (hexagonal array, perfect bond).

$$I_3 = \int_{L_k} \frac{(\tau - z_k)^m \,\mathrm{d}\tau}{(\tau - z)^n} = \begin{cases} 2\pi i \begin{pmatrix} m \\ n-1 \end{pmatrix} (z - z_k)^{m-n+1} & z \in D_k \\ 0 & z \notin D_k \cup L_k \\ \pi i (t - z_k)^m & z \in L_k,\ n = 1 \end{cases}$$

Appendix B. Stresses at internal points

The stresses $(\sigma_{xx})_k$, $(\sigma_{yy})_k$, and $(\sigma_{xy})_k$ inside the kth inclusion are

$$(\sigma_{xx})_k + (\sigma_{yy})_k = \frac{8\mu_k}{\kappa_k + 1} \mathrm{Re}\left\{ B_{0k}\left(a_{1k} - \frac{\alpha_k + \beta_k}{R_k}\right) + \sum_{m=1}^{M_{2k}} B_{mk}\left(a_{1k} - \frac{m+1}{R_k}\alpha_k\right) \Big/ F_{mk}(z) \right.$$
$$- \sum_{m=2}^{M_{1k}} \overline{B}_{-mk} \frac{m+1}{R_k} \beta_k / F_{mk}(z) - \sum_{\substack{j=1 \\ j \neq k}}^{N} \left[\sum_{m=2}^{M_{1j}} B_{-mj}\left(a_{1j} + \frac{m-1}{R_j}\alpha_j\right) F_{mj}(z) \right.$$
$$\left.\left. + \sum_{m=2}^{M_{2j}} \overline{B}_{mj} \frac{m-1}{R_j} \beta_j F_{mj}(z) \right] \right\} + \frac{\mu_k(\kappa + 1)}{\mu(\kappa_k + 1)} \left(\sigma_{xx}^{\infty} + \sigma_{yy}^{\infty}\right)$$

$$(\sigma_{yy})_k - (\sigma_{xx})_k + 2i(\sigma_{xy})_k = \frac{4\mu_k}{\kappa_k + 1} \left\{ \sum_{m=1}^{M_{2k}} B_{mk} \left[m\left(a_{1k} - \frac{m+1}{R_k}\alpha_k\right) \frac{1}{F_{(m-1)k}(z)\overline{F_{1k}(z)}} \right.\right.$$
$$\left. - (m-1)\left(a_{1k} - \frac{m+1}{R_k}\alpha_k - \frac{\beta_k}{R_k}\right) \Big/ F_{(m-2)k}(z) \right]$$
$$- \sum_{m=2}^{M_{1k}} \overline{B}_{-mk} \left[m \frac{m+1}{R_k} \beta_k \frac{1}{F_{(m-1)k}(z)\overline{F_{1k}(z)}} \right.$$
$$\left. + (m-1)\left(\frac{a_{3k} - a_{1k}}{m-1} - \frac{m+1}{R_k}\beta_k - \frac{\alpha_k}{R_k}\right) \Big/ F_{(m-2)k}(z) \right]$$
$$+ \sum_{\substack{j=1 \\ j \neq k}}^{N} \left[B_{0j}\left(a_{3j} - 2a_{1j} + 2\frac{\alpha_j + \beta_j}{R_j}\right) F_{2j}(z) \right.$$
$$- \overline{B}_{1j}\left(a_{1j} - a_{3j} - 2\frac{\alpha_j}{R_j}\right) F_{3j}(z) + \sum_{m=2}^{M_{1j}} B_{-mj}\left(m\left(a_{1j} + \frac{m-1}{R_j}\alpha_j\right) \frac{F_{(m+1)j}(z)}{\overline{F_{1j}(z)}} \right.$$
$$\left. - (m+1)\left(a_{1j} + \frac{m-1}{R_j}\alpha_j - \frac{\beta_j}{R_j}\right) F_{(m+2)j}(z) \right)$$
$$+ \sum_{m=2}^{M_{2j}} \overline{B}_{mj} \left(\left(a_{3j} - a_{1j} - (m-1)(m+1)\frac{\beta_j}{R_j} \right.\right.$$
$$\left.\left.\left. + (m+1)\frac{\alpha_j}{R_j}\right) F_{(m+2)j}(z) + m(m-1)\frac{\beta_j}{R_j}\frac{F_{(m+1)j}(z)}{\overline{F_{1j}(z)}} \right) \right] \right\}$$
$$+ \frac{\mu_k(\kappa + 1)}{\mu(\kappa_k + 1)} \left(\sigma_{yy}^{\infty} - \sigma_{xx}^{\infty} + 2i\sigma_{xy}^{\infty}\right) \tag{B.1}$$

and the stresses σ_{xx}, σ_{yy}, and σ_{xy} in the matrix are

$$\sigma_{xx}+\sigma_{yy}=-\frac{8\mu}{\kappa+1}\mathrm{Re}\left\{\sum_{j=1}^{N}\left[\sum_{m=2}^{M_{1j}}B_{-mj}\left(a_{1j}+\frac{m-1}{R_j}\alpha_j\right)+\sum_{m=2}^{M_{2j}}\overline{B}_{mj}\frac{m-1}{R_j}\beta_j\right]F_{mj}(z)\right\}+\sigma_{xx}^{\infty}+\sigma_{yy}^{\infty}$$

$$\begin{aligned}\sigma_{yy}-\sigma_{xx}+2i\sigma_{xy}=\frac{4\mu}{\kappa+1}\sum_{j=1}^{N}\Bigg\{&B_{0j}\left(a_{3j}-2a_{1j}+2\frac{\alpha_j+\beta_j}{R_j}\right)F_{2j}(z)-\overline{B}_{1j}\left(a_{1j}-a_{3j}-2\frac{\alpha_j}{R_j}\right)F_{3j}(z)\\&+\sum_{m=2}^{M_{1j}}B_{-mj}\left[m\left(a_{1j}+\frac{m-1}{R_j}\alpha_j\right)\frac{F_{(m+1)j}(z)}{\overline{F_{1j}(z)}}-(m+1)\left(a_{1j}+\frac{m-1}{R_j}\alpha_j-\frac{\beta_j}{R_j}\right)F_{(m+2)j}(z)\right]\\&+\sum_{m=2}^{M_{2j}}\overline{B}_{mj}\left[\left(a_{3j}-a_{1j}-(m-1)(m+1)\frac{\beta_j}{R_j}+(m+1)\frac{\alpha_j}{R_j}\right)F_{(m+2)j}(z)\right.\\&\left.+m(m-1)\frac{\beta_j}{R_j}\frac{F_{(m+1)j}(z)}{\overline{F_{1j}(z)}}\right]\Bigg\}+\sigma_{yy}^{\infty}-\sigma_{xx}^{\infty}+2i\sigma_{xy}^{\infty}\end{aligned}\tag{B.2}$$

References

Aboudi, J., 1987. Damage in composites—modeling of imperfect bonding. Composites Science and Technology 28, 103–128.

Achenbach, J.D., Zhu, H., 1989. Effect of interfacial zone on mechanical behavior and failure of fiber-reinforced composites. Journal of the Mechanics and Physics of Solids 37, 381–393.

Achenbach, J.D., Zhu, H., 1990. Effect of interphases on micro and macromechanical behavior of hexagonal-array fiber composites. Journal of Applied Mechanics 57, 956–963.

Barnes, R., Janković, I., 1999. Two-dimensional flow through large numbers of circular inhomogeneities. Journal of Hydrology 226, 204–210.

Bigoni, D., Serkov, S.K., Valentini, M., Movchan, A.B., 1998. Asymptotic models of dilute composites with imperfectly bonded inclusions. International Journal of Solids and Structures 35, 3239–3258.

Brebbia, C.A., Telles, J.C.F., Wrobel, L.C., 1984. Boundary Element Techniques: Theory and Applications in Engineering. Springer-Verlag, Berlin.

Chen, T., 2001. Thermal conduction of a circular inclusion with variable interface parameter. International Journal of Solids and Structures 38, 3081–3097.

Crouch, S.L., Mogilevskaya, S.G., 2002. On the use of somigliana's formula and Fourier series for elasticity problems with circular boundaries. International Journal for Numerical Methods in Engineering, submitted for publication.

Gao, Z., 1995. A circular inclusion with imperfect interface: Eshelby's tensor and related problems. Journal of Applied Mechanics 62, 860–866.

Golub, G.H., Van Loan, C.F., 1996. Matrix Computation. J. Hopkins University Press, Baltimore.

Gong, S.X., Meguid, S.A., 1993. Interacting circular inhomogeneities in plane elastostatics. Acta Mechanica 99, 49–60.

Hashin, Z., 1990. Thermoelastic properties of fiber composites with imperfect interface. Mechanics of Materials 8, 333–348.

Hashin, Z., 1991. The spherical inclusion with imperfect interface. Journal of Applied Mechanics 58, 444–449.

Janković, I., 1997. High-order analytic elements in modeling groundwater flow. Ph.D. Thesis. University of Minnesota, Minneapolis.

Jasiuk, I., Kouider, M.W., 1993. The effect of an inhomogeneous interphase on the elastic constants of transversely isotropic composites. Mechanics of Materials 15, 53–63.

Jun, S., Jasiuk, I., 1993. Elastic moduli of two-dimensional composites with sliding inclusions—A comparison of effective medium theories. International Journal of Solids and Structures 30, 2501–2523.

Linkov, A.M., Mogilevskaya, S.G., 1994. Complex hypersingular integrals and integral equations in plane elasticity. Acta Mechanica 105, 189–205.

Linkov, A.M., Mogilevskaya, S.G., 1995. On the theory of complex hypersingular equations. In: Proceedings of the International Conference on Computational Engineering Science. Springer-Verlag, Berlin, pp. 2836–2840.

Mogilevskaya, S.G., 1996. The universal algorithm based on complex hypersingular integral equation to solve plane elasticity problems. Computational Mechanics 18, 127–138.

Mogilevskaya, S.G., Crouch, S.L., 2001. A Galerkin boundary integral method for multiple circular elastic inclusions. International Journal for Numerical Methods in Engineering 52, 1069–1106.

Muskhelishvili, N.I., 1959. Some Basic Problems of the Mathematical Theory of Elasticity. Noordhoff, Groningen, The Netherlands.

Ru, C.Q., 1998. A circular inclusion with circumferentially inhomogeneous sliding interface in plane elastostatics. Journal of Applied Mechanics 65, 30–38.

Ru, C.Q., 1999. A new method for an inhomogeneity with stepwise graded interphase under thermomechanical loadings. Journal of Elasticity 56, 107–127.

Ru, C.Q., Schiavone, P., 1997. A circular inclusion with circumferentially inhomogeneous interface in antiplane shear. Proceedings of the Royal Society of London A 453, 2551–2572.

Strack, O.D.L., 1989. Groundwater Mechanics. Prentice-Hall, Englewood Cliffs, NJ.

Sudak, L.J., Ru, C.Q., Schiavone, P., Mioduchowski, A., 1999. A circular inclusion with inhomogeneously imperfect interface in plane elasticity. Journal of Elasticity 55, 19–41.

Wang, J., Mogilevskaya, S.G., Crouch, S.L., 2001. A Galerkin boundary integral method for nonhomogeneous materials with cracks. In: Proceedings of the 38th Rock Mechanics Symposium, Washington, DC, pp. 1453–1460.